DISCLAIMER

This report was prepared as an account of work sponsored by an agency of the United States Government. Neither the United States Government nor any agency thereof, nor any of their employees, makes any warranty, express or implied, or assumes any legal liability or responsibility for the accuracy, completeness, or usefulness of any information, apparatus, product, or process disclosed, or represents that its use would not infringe privately owned rights. Reference herein to any specific commercial product, process, or service by trade name, trademark, manufacturer, or otherwise does not necessarily constitute or imply its endorsement, recommendation, or favoring by the United States Government or any agency thereof. The views and opinions of authors expressed herein do not necessarily state or reflect those of the United States Government or any agency thereof. Reference herein to any social initiative (including but not limited to Diversity, Equity, and Inclusion (DEI); Community Benefits Plans (CBP); Justice 40; etc.) is made by the Author independent of any current requirement by the United States Government and does not constitute or imply endorsement, recommendation, or support by the United States Government or any agency thereof.

LA-UR-25-25454

Title:	Predicting Thermoset Resin Cure Kinetics for Composite Processing
Author(s):	Pace, Alexandra Elizabeth Chov, Ashleigh Meyjin
Intended for:	Report
Issued:	2025-06-09

Los Alamos
NATIONAL LABORATORY

Predicting Thermoset Resin Cure Kinetics for Composite Processing

Lexie Pace[1,2], Ashleigh Chov[2]

[1]Knight Campus Graduate Internship Program, University of Oregon; [2]Los Alamos National Laboratory

CH 601: Polymer Internship Research Credits (Spring 2025)

Kinetic parameters; Activation energy; Pre-exponential factor; Epoxy, resole phenol, cyanate ester resins

---

Predicting a material's thermal properties is not only useful for designing parts but also for defining processing parameters. This is especially applicable to wet-filament winding operations and the production of composite parts using thermoset resins. For these, the formation of cross-linking bonds is affected by time and temperature, but the degree of cross-linking can be modeled using phenomenological methods. In the current study, the Kissinger and Flynn/Wall/Ozawa methods were both used to calculate kinetic parameters and produced values that were in agreement with each other. The kinetic parameters activation energy (E_a) and pre-exponential factor (A) calculated from exothermic peak data increased between an epoxy and resole phenol resin system, with a cyanate ester having the highest. The successful application of both methods suggests applicability to future studies for developing cure recipes.

INTRODUCTION

In filament winding, fibers impregnated with resin are laid down in a predetermined pattern to optimize strength and weight distribution in composite parts.[1] Due to the nature of the process, there are limitations to the materials that may be utilized. For example, resins with long gel times (≥20 hr for a 30g mass at 25°C)[2] and low viscosity (1000 cPoise at 25°C[2] or at most 800-2000 cP) are ideal for wet-filament winding (WFW), though potential fiber slippage due to the low viscosity should be sufficiently addressed in the fiber layup design.[3]

Knowledge of how in-process, as well as post-cured, material properties change with environmental conditions is necessary for the fabrication and design of composite parts. For thermoset resins, time and temperature affect the degree of cure or extent of cross-linking. The curing process, a series of chemical reactions that elongate the polymer chains and build the network of molecules, can be modeled with the general rate equation, Eqn. (1):

$$\frac{d\alpha}{dt} = k(T) \cdot f(\alpha) \tag{1}$$

where $(d\alpha/dt)$ is the conversion rate (α is the degree of cure or conversion), $k(T)$ is the reaction rate coefficient, and $f(\alpha)$ is the conversion function. Substitution with the Arrhenius equation simplifies this expression to Eqn. (2):

$$\frac{d\alpha}{dt} = A\ exp\left({}^{-E_a}/_{RT}\right) \cdot f(\alpha) \tag{2}$$

An n^{th} order chemical reaction may therefore be modeled using Eqn. (3):

$$\frac{d\alpha}{dt} = A\ exp\left({}^{-E_a}/_{RT}\right) \cdot (1-\alpha)^n \tag{3}$$

This provides a means for estimating kinetic parameters, such as the activation energy (E_a) and the pre-exponential factor (A), using the gas constant (R) and information from thermal analyses. It is then possible to predict the progression of cure during a specified temperature program (i.e., cure recipe) with this information (see Figure 1 for an example)[4] to aid in understanding in-process characteristics and defining process control methods.

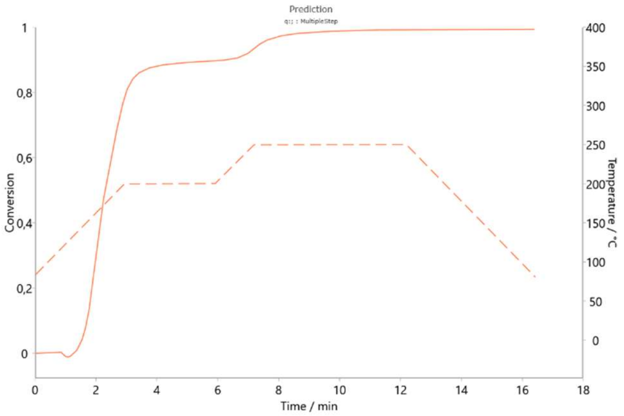

Figure 1. Prediction of cure conversion (solid line) over a defined temperature program (dashed line) using DSC results and Kinetics Neo software.

Estimation of kinetic parameters in this way is a phenomenological method useful for when the fundamental chemical process is difficult to define, such as with resin systems, which make the mechanistic approach challenging.[5] The phenomenological method also utilizes standard thermal analysis techniques conducted dynamically or isothermally at a variety of heating rates (β) or temperatures (T), respectively, and a multitude of strategies have been proposed to exploit those results in order to approximate the aforementioned kinetic parameters.[6]

Beyond kinetic parameters, there are many other factors that should be considered in composite part design.

Material compatibility (i.e., adhesion of the resin to the fiber), storage and preparation requirements, and impregnation system (i.e., bath or metered application) impact mechanical properties. Quality control, cost savings, and end-use properties can also be affected by allowable winding speed and cycle time.[3,7] The consolidation method (i.e., compaction during cure) is another factor that influences material choice. During this process, the ability to remove trapped air and other volatiles as well as control fiber volume is largely dependent on resin viscosity.

Curing in an autoclave is an option that provides increased heat transfer to tools and parts due to the pressurized nitrogen media and easily meets exacting process specifications.[8] This method however, incurs not only large start-up costs but also extensive operational and time requirements. Vacuum-bag or Out-of-Autoclave processing is a less expensive alternative, though greater consideration of "debulk schedules, breather types, air path methods, lay up materials, resin rheology, ramp rates, temperature and time"[9] is necessary to achieve comparable results. Additional factors, such as part geometry as well as post-processing operations (i.e., removal of excess resin) and finish requirements may also dictate its implementation.[10]

-- GENERAL RESIN PROPERTIES--

Epoxies, resole phenolics, and cyanate esters are potential resin systems for WFW applications. Epoxy resins are strong as well as thermally and chemically resistant with good adhesive properties. A common epoxy system utilizes the instability of the epoxide ring to create the cross-linked network with amines (see Figure 2).[11] A drawback to epoxies is its tendency to off-gas volatile substances.[12] This creates challenges in the manufacturing process and also increases the possibility of porosity in the cured material, which would compromise the part's integrity. Part design and material selection for epoxy-based components must therefore consider operating conditions that could exacerbate porosity, such as reduced pressure.[12] A post-cure step at an elevated temperature after curing at ambient temperatures could mitigate this risk .[13]

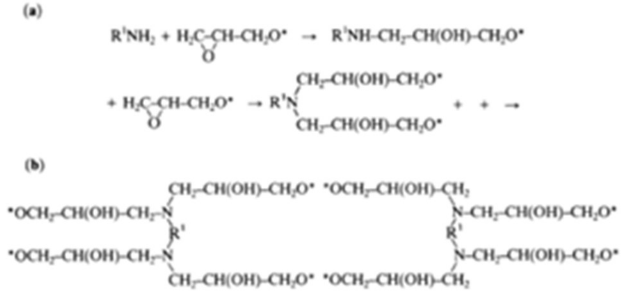

Figure 2. Ethylene amine and epoxy resin curing reaction; (a) amine (b) diamine.

Phenolic resins have high strength as well as good dimensional stability and chemical resistance at high temperatures. Phenolics start as a prepolymer made from a 1.2 – 3.0 : 1 mixture of formaldehyde : phenol in alkaline conditions. The prepolymer is then cured by heating to elevated temperatures; cross-linking occurs via condensation reactions to form methylene and ether bridges between benzene rings (see Figure 3)[14] and does not require a curing agent. A disadvantage of phenolics is their volatile content and tendency to off-gas, not only from unreacted reagents but also water and other volatile substances generated during the curing process,[15,16] similar to epoxies.

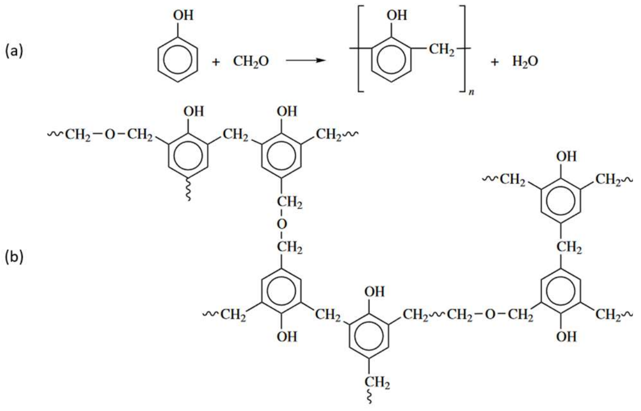

Figure 3. Resole phenolic condensation reaction (a) resulting in network structure with methylene and ether bridges (b).

Cyanate ester resins have good thermo-oxidative and dimensional stability along with low shrinkage and off-gassing tendencies. The network is cross-linked with triazines built via cyclotrimerization of the cyanate end groups (see Figure 4)[17] at high temperatures using a curing agent containing a cobalt acetylacetonate metal coordination catalyst and nonylphenol co-catalyst to improve solubility.[17,18] To reduce cost and improve toughness, modification with an epoxy copolymer is common.

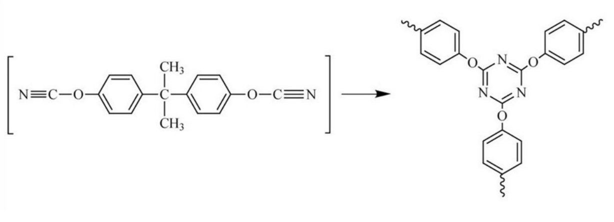

Figure 4. Cyclotrimerization reaction of bisphenol A dicyanate to form triazine network structure.

EXPERIMENTAL

--MATERIALS--

A one-part resole phenol resin sample was supplied by SBHPP / Durez (product number 34585) and a two-part epoxy and cyanate ester were supplied by Epic Resins (product number R3500/H5016) and Toray (product number RS-16), respectively. The liquid samples were prepared according to the manufacturer's directions, if required.

--CHARACTERIZATION METHODS--

A TA Instruments TGA Q500 was utilized at a variety of heating rates (reference Table 1) to study weight loss.

Table 1. Resin types, supplier, and testing parameters for TGA and DSC characterization.

Resin System	Product Name	Mfg.	TGA Avg Sample Size [mg]	TGA Heating Rates [°C/min]	DSC Avg Sample Size [mg]	DSC Heating Rates [°C/min] *results not included
Epoxy (two-part)	R3500/H5016	Epic Resins	N/A	N/A	18.98 ± 2.49	5, 7, 10, 15, 20
Phenol Resole (one-part)	34585	Durez / SBHPP	4.89 ± 0.22	2.5, 5, 7, 10, 15, 20	2.72 ± 0.63	1, 3, 5, 7, 10*, 20*
Cyanate Ester (two-part)	RS-16	Toray	6.74 ± 1.75	2.5, 5, 7, 10, 15, 20	8.07 ± 1.45	1, 2.5*, 3, 5, 7, 10, 20

Samples were also tested in Tzero hermetically sealed aluminum pans (phenolic Durez 34585 required modification with a pinhole to account for volatiles from the condensation reaction) on a TA Instruments Discovery DSC 2500 at a variety of heating rates (reference Table 1) to study changes in enthalpy. Analyses were performed using TA Universal Analysis and TRIOS software.

--ANALYTICAL APPROACHES--

A number of standard methods were consulted for the selection of testing parameters and analytical techniques: ASTM E1641 – 23: Standard Test Method for Decomposition Kinetics by Thermogravimetry Using the Ozawa/Flynn/Wall Method; ASTM E537 - 24: Standard Test Method for Thermal Stability of Chemicals by Differential Scanning Calorimetry; ASTM E2890 - 21: Determination of Kinetic Parameters and Reaction Order for Thermally Unstable Materials by Differential Scanning Calorimetry Using the Kissinger and Farjas Methods; ASTM E698 – 23: Standard Test Method for Kinetic Parameters for Thermally Unstable Materials Using Differential Scanning Calorimetry and the Flynn/Wall/Ozawa Method; ASTM E2041 – 23: Standard Test Method for Estimating Kinetic Parameters by Differential Scanning Calorimeter Using the Borchardt and Daniels Method.

It is noted in ASTM E1641 that studies of reactions involving volatiles may be less reliable at high heating rates where α of those volatiles may become the rate-controlling process and affect decomposition kinetics.[19] It is also noted in ASTM E537, that when using small quantities of material, the headspace volume to sample size is large and any vaporization effects could skew results; headspace gas may also impact the evaluation if considered reactive in the system being studied.[20] These considerations are relevant to the study of the phenolic Durez 34585 resin which produces volatiles when cured and contains 1-2% reactive ethylene glycol[19] but no adjustments were made to account for these phenomena in the results.

RESULTS & DISCUSSION

--TGA--

Weight change analysis of the thermogravimetric thermograms from a variety of heating rates (see Figure 5 for phenolic Durez 34585 results) was conducted. To achieve a similar α, a higher temperature needed to be reached when heated at higher rates compared to lower. Similarly, more weight loss was seen at lower heating rates compared to higher at a constant temperature as more energy was absorbed during the longer heating time. TGA testing was not performed on epoxy samples.

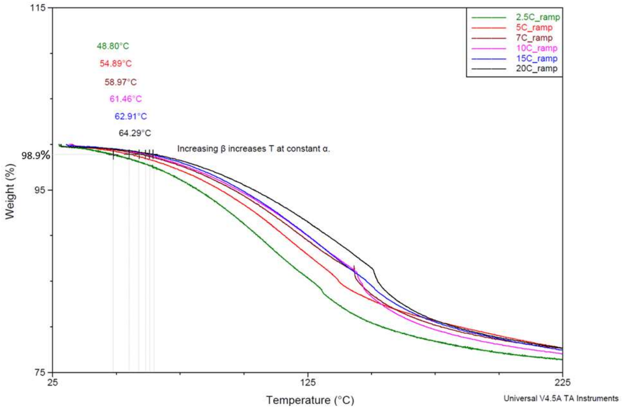

Figure 5. Thermogravimetric thermograms of phenolic Durez 34585 samples depicting temperatures required to achieve 5% conversion (ie weight loss) during the condensation reaction that results in ~20% loss of the initial weight at varying heating rates.

From these results, the relationship between $log\beta$ and $\frac{1}{T}$ at different α was found (see Figure 6 for phenolic Durez 34585 results) and used to estimate an initial activation energy (E') with the Flynn/Wall/Ozawa (FWO) method and Eqn. (4):

$$E' = -\frac{R}{b} \cdot \frac{d(log\beta)}{d(1/T)} \qquad (4)$$

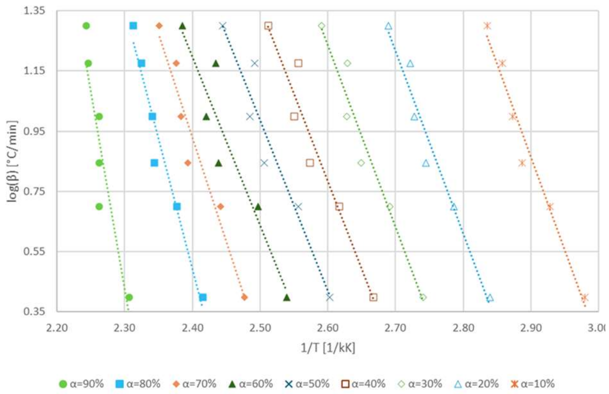

Figure 6. Linear regression of phenolic Durez 34585 TGA results based on the FWO method.

where b is the Doyle approximation constant. Following ASTM E1641, E' was then refined using a new b value in Eqn. (4) found from the table published in the standard after calculating E'/RT; the T used was the measured temperature at the applicable α for the setting in the middle of the range of tested conditions (ie 5°C/min). This method is a way to study decomposition reactions, and it is assumed that the curing of phenolic resin through a condensation reaction is such and can be studied in this manner. A treated resin reacts differently than uncured therefore this study may only be applicable to how a material performs instead of how it can be processed.

The iterative process continued until the change in the recalculated value of E' was less than 1% and is reported as the final E_a (results are outlined in Table 2). This may not be necessary if a value of b is selected ahead of time, as seen in the study by Zhang et al.[16] The E_a found in the final iteration of the above refinement process was then used to calculate A with Eqn. (5):

Table 2. Kinetic parameters for different resin types calculated using various methods.

Resin System	E_a [kJ/mol]	A [1/sec]
Epic Epoxy	TGA: - DSC: 53.51 ± 4.54 (Kissinger) 53.5 (FWO)	TGA: - DSC: 1.82E+05 (Kissinger) 1.64E+05 (FWO)
Phenol Durez 34585	TGA: 106.41 ± 5.09 DSC: 96.27 ± 1.57 (Kissinger) 96.21 (FWO)	TGA: 2.45E+12 DSC: 7.18E+09 (Kissinger) 6.88E+9 (FWO)
Cyanate Ester Toray RS-16	TGA: 208.72 ± 3.46 DSC: 119.01 ± 4.59 (Kissinger) 118.9 (FWO)	TGA: 1.76E+13 DSC: 1.84E+12 (Kissinger) 1.92E+12 (FWO)

$$A = (-\beta R/E_a) \cdot ln\,(1-\alpha) \cdot 10^a \qquad (5)$$

where β and T are again from the middle of the range of tested conditions (ie 5°C/min) at the applicable α and a is the Doyle approximation constant taken from the table in the standard.

Little variability was seen in the kinetic parameters for α values less than 0.6 (see Figure 7 for phenolic Durez 34585 results). Similar to results reported by Zhang et al., an exponential increase in E_a occurred during the end of the cure and may be due to the higher viscosity in the latter stages where diffusion becomes the rate-controlling step. Zhang however, reported a dependence when α<0.6, describing E_a's initial linear increase to be due to the volatilization of free molecules[16] compared to the roughly independent relationship found in this study. ASTM E1641 notes that volatile, low-level impurities affect low conversion results, thus an explanation for the difference could be in the raw material formulation and solvent used.

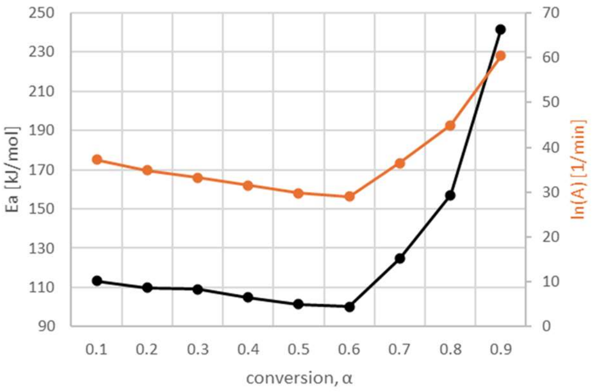

Figure 7. Consistency of kinetic parameters throughout cure of phenolic Durez 34585 using TGA results based on the FWO method.

--DSC--

Exothermic peak analysis of the differential thermograms from a variety of heating rates showed the expected results that increasing β caused an increase in both the peaks' max temperature (T_p) and slope[5] (see Figure 8 for phenolic Durez 34585 results). Sigmoidal horizontal integration was

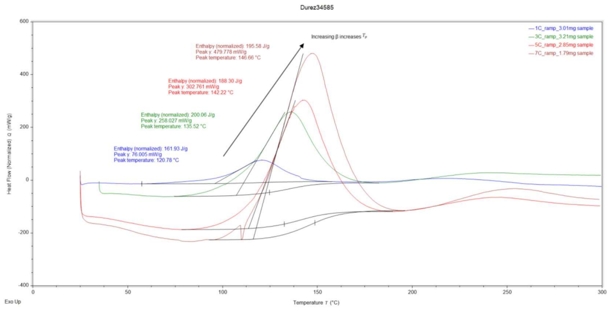

Figure 8. Differential thermograms of phenolic Durez 34585 depicting onset and peak temperatures, maximum heat flow and total enthalpy measured at varying heating rates.

performed during the analyses of the phenolic samples compared to a linear integration for the cyanate ester and epoxy samples, as seen in Figure 9. This was because a change in the baseline was observed after the transition, potentially due to the sample weight decreasing because of volatilization, and this method also corrects for the change in heat capacity that results from curing.[21,22] Only the first exothermic peak around 150°C in the phenolic results was analyzed. The shoulder present in the cyanate ester results is attributed to the competing autocatalytic reaction of the uncatalyzed portion of resin,[23,24] the further polymerization made possible when the T_g is exceeded to overcome vitrification and diffusion limitations,[25,26] and/or is an indication of multiple reaction pathways occurring successively.[27]

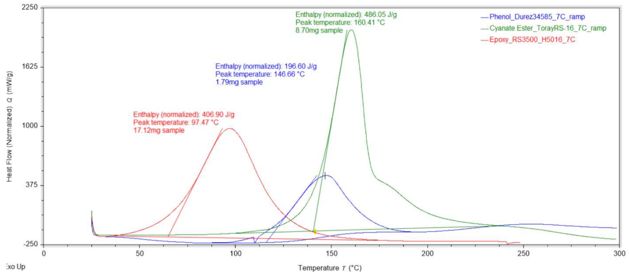

Figure 9. Comparison of the differential thermograms from the different resins tested at 7°C/min; sigmoidal integration was conducted on phenolic Durez 34585 samples due to the change in baseline.

After correcting the observed peak temperature (T) according to ASTM E2890 with Eqn. (6):[28]

$$T_p = T + \varphi \cdot q_{max} \tag{6}$$

where q_{max} is the maximum heat flow measured at T and φ is the thermal resistance determined from a calibration with indium, the relationship between $ln\left(\frac{\beta}{T_p^2}\right)$ and $\frac{1}{T_p}$ at i different β's was found using the Kissinger method and Eqn. (7):

$$ln\left(\frac{\beta_i}{T_{p,i}^2}\right) = ln\left(\frac{AR}{E_a}\right) - \frac{E_a}{RT_{p,i}} \tag{7}$$

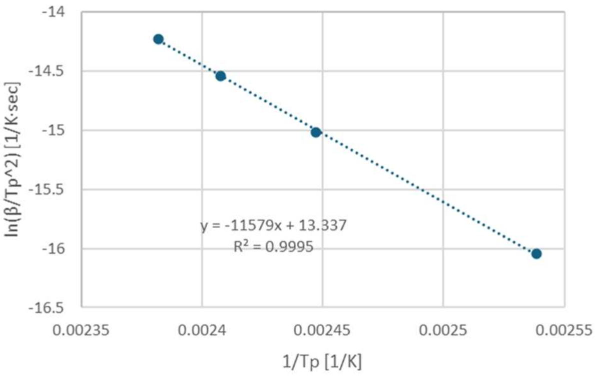

Figure 10. Linear regression results from the Kissinger method for phenolic Durez 34585 using DSC results.

that was then used to estimate E_a and A[6] (see Figure 10 for phenolic Durez 34585 results). The Kissinger method assumes that the maximum curing rate occurs at T_p since the rate of heat evolution during exothermic behavior is proportional to $d\alpha/dt$.

Similarly, a relationship between lnβ and $\frac{1}{T_p}$ was found (see Figure 11 for phenolic Durez 34585 results). Following the procedure outlined by Zhou et al.,[29] that uses the reduced Crane method, with the E_a found from the Kissinger method above and Eqn. (8):

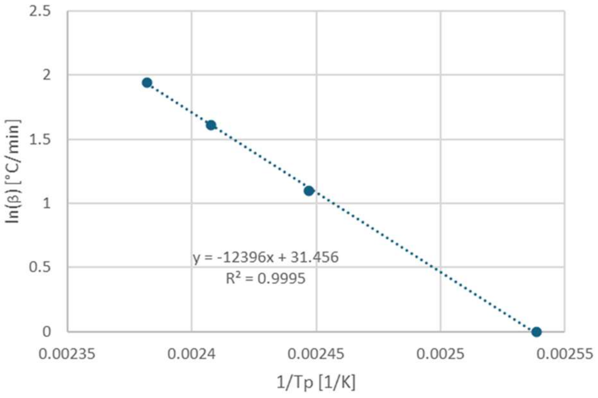

Figure 11. Linear regression of phenol Durez 34585 DSC results based on Zhou et al.9 and the Crane method.

$$\frac{d(ln\beta)}{d(1/T_p)} = -\frac{E_a}{nR} \tag{8}$$

an estimate of the reaction order (n) was made to define an explicit rate equation of the form shown in Eqn. (3).

Calculations resulted in 0.9 < n < 1.1 for all three resins tested, therefore the reactions were approximated as first-order reactions, simplifying Eqn. (3) so that its integral form becomes Eqn. (9):[29]

$$t = \frac{-ln(1-\alpha)}{Aexp(-E_a/RT)} \tag{9}$$

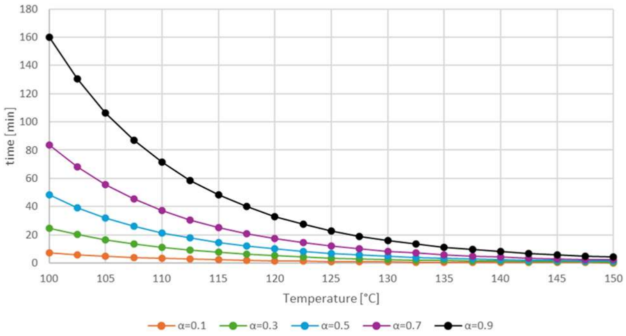

Figure 12. Cure time dependence on temperature at different conversions (α) for phenolic Durez 34585.

from which the dependence of curing time on temperature was calculated for different α values (see Figure 12 for phenolic Durez 34585 results). This shows that a reduction in reaction temperature will result in a lower degree of cure unless the reaction time is increased.

Similarly, the dependence of conversion on cure time at different temperatures was calculated using Eqn. (10) (see Figure 13 for phenolic Durez 34585 results):

$$\alpha = 1 - exp\,[-A \cdot t \cdot exp(-E_a/RT)] \qquad (10)$$

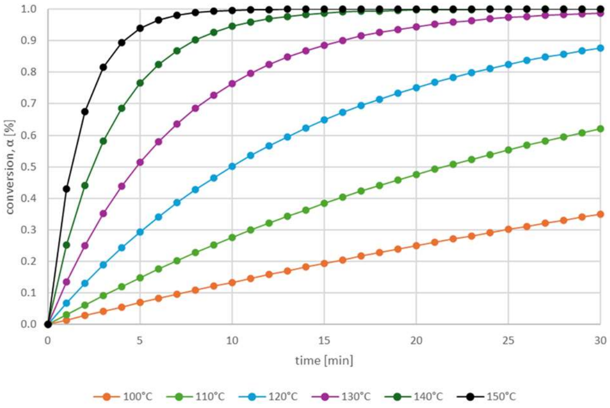

Figure 13. Cure conversion dependence on time at different temperatures for phenolic Durez 34585.

Here it is seen that a reduction in reaction time requires a higher reaction temperature for an equivalent degree of cure.

The effect of both time and temperature on conversion can also be displayed as in Figure 14 to visually compare different systems. The higher value of E_a for the cyanate ester system results in the need for longer reaction times and/or higher temperatures to achieve a comparable degree of cure to the epoxy and phenolic systems. The changes in slope also provide a visualization of the different stages in the curing process. Initially, the cure is slow due to the limited amount of radicals that enable bond formation. Then the rate increases to a maximum as more bonds are formed. Finally, the high degree of crosslinking decreases the rate due to the increase in viscosity limiting the mobility of reactants.

Time and temperature in a nonisothermal reaction are related through the heating rate (β) so Eqn. (10) can be rewritten as Eqn. (11):

$$\alpha = 1 - exp\,[-A \cdot \frac{T - T_o}{\beta} \cdot exp(-E_a/RT)] \qquad (11)$$

where T_o is the initial temperature. From this, the dependence of conversion on temperature for different heating rates was calculated (see Figure 15 for phenolic Durez 34585 results). To achieve the same degree of cure, a higher heating rate will have to reach a higher temperature compared to a lower heating rate.

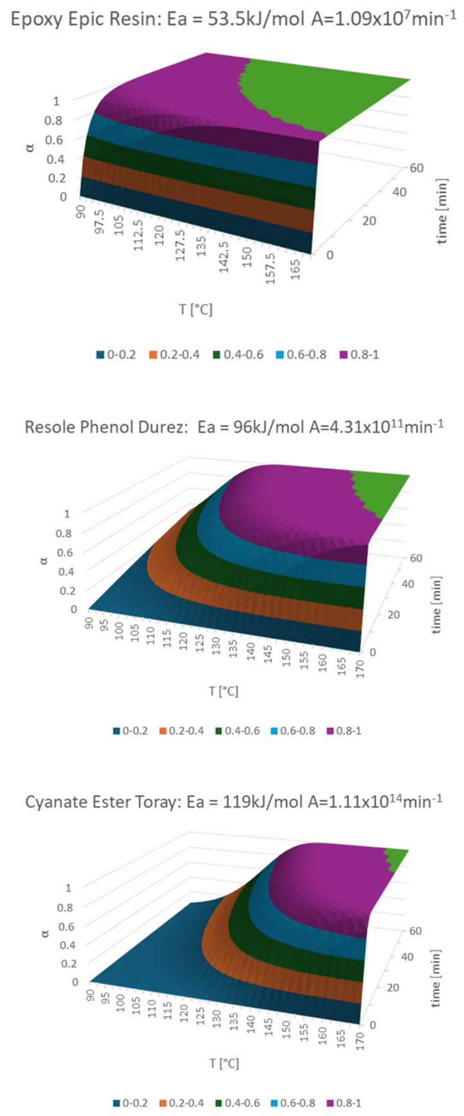

Figure 14. A visual comparison of the effects of time and temperature on the degree of cure for epoxy (top), resole phenol (middle), and cyanate ester (bottom) resin systems.

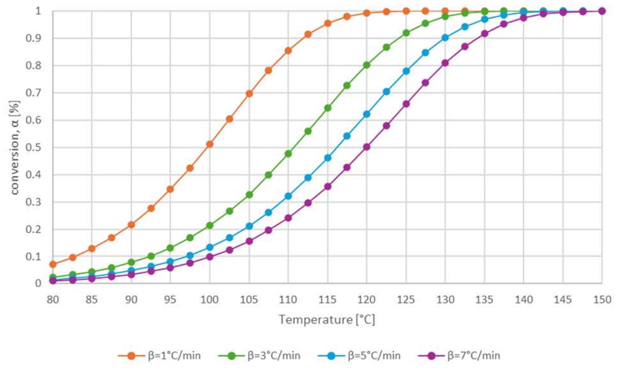

Figure 15. Cure conversion dependence on temperature at different heating rates for phenolic Durez 34585; To = 50°C.

In a similar manner, the dependence of conversion on time for different heating rates was calculated using Eqn. (12) (see Figure 16 for phenolic Durez 34585 results):

$$\alpha = 1 - exp\left[-A \cdot t \cdot exp\left(\frac{-E_a}{R \cdot [T_o + \beta \cdot t]}\right)\right] \qquad (12)$$

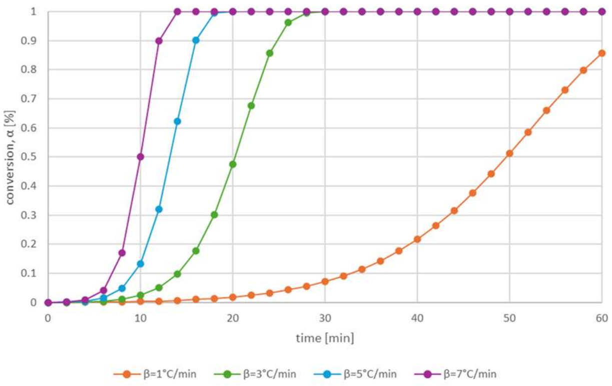

Figure 16. Cure conversion dependence on time at different heating rates for phenolic Durez 34585; To = 50°C.

Here, longer reaction time is required at lower heating rates to achieve the same degree of cure.

Similar to the Kissinger method, the observed peak temperature was corrected according to ASTM E698 and the FWO method to account for the difference between the temperatures of the specimen and that of the external sensor in the instrument. The relationship between $\log_{10}\beta$ and $\frac{1}{T_p}$ was found to estimate an initial value of E' (see Figure 17 for phenolic Durez 34585 results) using Eqn. (13):[30]

$$E' = -2.19 \cdot R \cdot \left[\frac{d(log_{10}\beta_i)}{d(1/T_{p,i})}\right] \qquad (13)$$

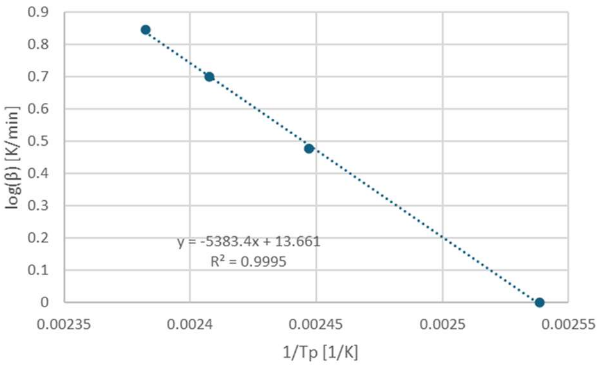

Figure 17. Linear regression results from the FWO method for phenolic Durez 34585 using DSC results.

Following ASTM E698, E' was then refined using Eqn. (14):

$$E = \left(-2.303\frac{R}{D}\right) \cdot \left[\frac{d(log_{10}\beta)}{d(1/T_p)}\right] \qquad (14)$$

where D is a constant published in the standard for multiple values of E/RT that was calculated using the T_p measured at the setting in the middle of the range of tested conditions (ie 10, 3 and 5°C/min for Epic, Durez, and Toray, respectively). If a recalculation of E/RT using the new value of E resulted in a significantly different D, E was again refined using Eqn. (14) with the new D. This process continued until little change in D was observed, from which the final E_a value was reported (results are outlined in Table 2).

The E_a found in the final iteration of the above refinement process was then used to calculate A, assuming a 1st order reaction, using Eqn. (15):

$$A = \frac{\beta \cdot E_a \cdot e^{E_a/RT}}{R \cdot T^2} \qquad (15)$$

where β and T are again from the middle of the range of tested conditions.

The values of E_a and A were verified in an aging test[30] by using the Arrhenius equation (see Eqn. (2)) to calculate the rate constant (k) at various temperatures. The isothermal aging time (t) was then determined using Eqn. (16):

$$t = \frac{0.693}{k} \qquad (16)$$

A sample was treated at the temperature that resulted in a t of at least one (1) hour for that amount of time, quenched to room temperature, then heated at a constant rate to analyze the residual reaction peak. Results from aging Toray RS-16 resin supported the previously calculated values as peak area and height of the aged sample were 59% and 52%, respectively, of an unaged sample (see Figure 18); approximately 50% was expected. The aging of the Durez 34585 resin however, resulted in values of about 35% for both peak area and height. The disparity may be an indication of the limitations of this method for modeling the phenolic system. Aging of the epoxy resin was not performed.

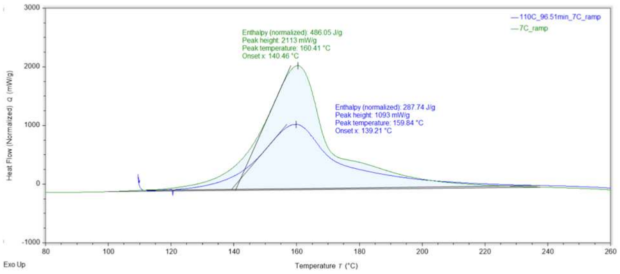

Figure 18. Comparison of reaction peaks from a cyanate ester Toray RS-16 resin sample aged at 110°C for 96.51min confirming estimations of Ea and A parameters per ASTM E698.

Degree of cure, α, may also be defined by Eqn. (17):[31]

$$\alpha(T) = \frac{\Delta H(T)}{\Delta H_{total}} \qquad (17)$$

where $\Delta H(T)$ is the heat evolved up to temperature T and ΔH_{total} is the total heat evolved during the reaction (Figure 19 shows results for phenolic Durez 34585); the rate of heat evolution is proportional to the rate of the chemical reaction, therefore integration of the heat flow with respect to time yields the heat of reaction. Lower heating rates were

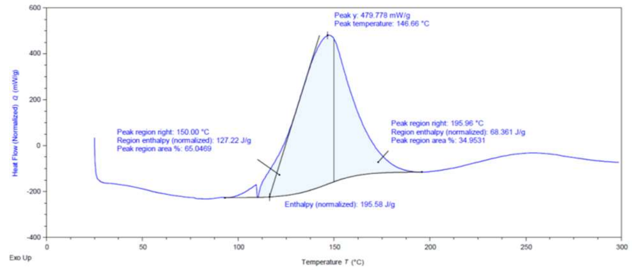

Figure 21. Differential thermogram of phenolic Durez 34585 tested at 7°C/min depicting partial heat evolved up to 150°C and the corresponding percentage of the total enthalpy.

found to achieve higher α at a set temperature. This trend was similar to the α values calculated using E_a in Eqn. (11) discussed previously. Results from the E_a calculation were found to be shifted to lower temperatures compared to those using ΔH (Figure 20 shows results for phenolic Durez 34585).

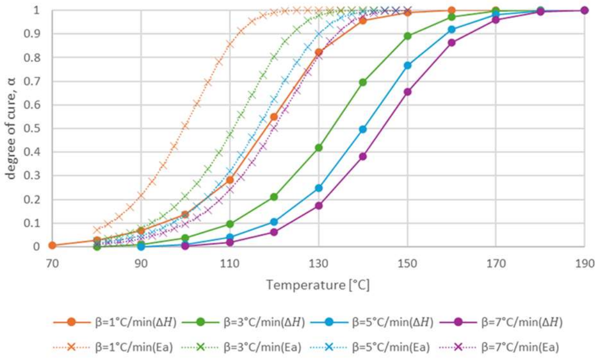

Figure 19. Degree of cure progression at different heating rates for phenolic Durez 34585 calculated using Ea with Eqn. (11) [dashed lines/'x' marker] and ΔH with Eqn. (17) [solid lines/'•' marker].

Table 3. Kinetic parameters calculated using the Borchardt and Daniels method.

Resin System	β [°C /min]	E_a [kJ/mol]	A [$1/sec$]
Phenol Durez 34585	1	143.07 ± 4.16	3.88E+16
	3	143.77 ± 4.13	2.92E+16
	5	224.94 ± 21.72	3.59E+26
	7	192.47 ± 6.64	1.84E+22
	AVG	**176.06**	**8.98E+25**
Cyanate Ester Toray RS-16	1	205.24 ± 11.40	1.59E+24
	3	163.49 ± 17.43	5.49E+18
	5	121.32 ± 16.71	4.39E+15
	7	123.09 ± 16.38	7.14E+15
	AVG	**153.28**	**3.96E+23**

The use of ΔH to calculate α was also accomplished by finding the relationship between $ln[k(T)]$ and $\frac{1}{T}$ using the Borchardt and Daniels method and Eqn. (18):

$$ln[k(T)] = ln\left(\frac{d\alpha}{dt}\right) - nln(1-\alpha) \qquad (18)$$

where $(d\alpha/dt)$ is the rate of reaction and $(1-\alpha)$ is the fraction remaining. Data from the exothermic peaks, illustrated in Fig. (21),[32] was taken at qty. ten (10) equally-spaced values between 10% and 90% of the total peak area following the procedure outlined in ASTM E2041. A line-of-best-fit was found by adjusting the value of $0 < n < 2$ in Eqn. (18) (see Figure 22 for phenolic Durez 34585 results). As the Arrhenius equation may be used to define $k(T)$, as seen in Eqn. (2), E_a and A parameters were calculated from the slope and intercept, respectively, of the regression results for each β. Significant variation in the calculated parameters across β was found (see Table 3); it is noted in ASTM E2041 that this method of analyzing data is only applicable to

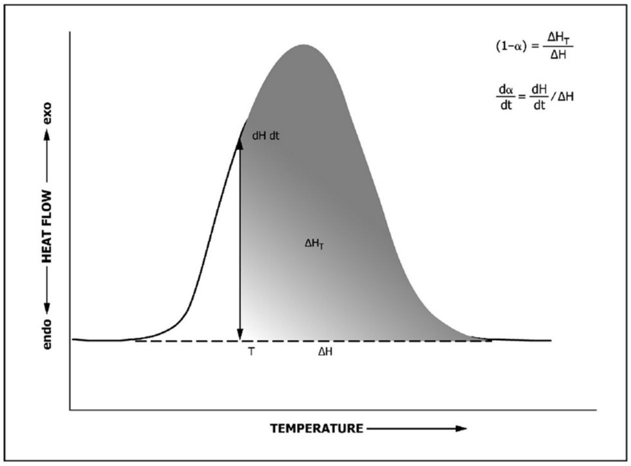

Figure 22. Illustration depicting values taken from an exothermic peak used to perform Borchardt and Daniels method calculations.

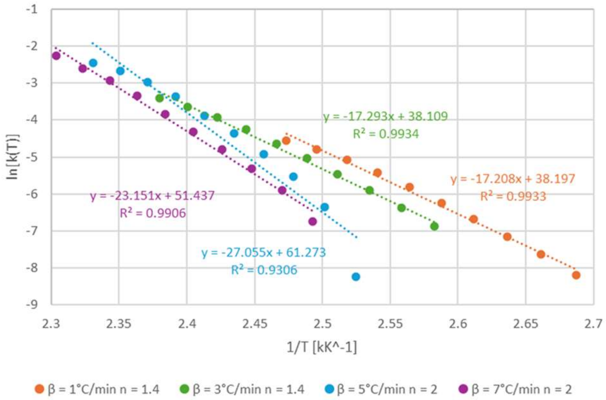

Figure 20. Linear regression of phenolic Durez 34585 DSC results based on the Borchardt and Daniels method.

reactions with a constant mechanism that results in smooth, well-shaped exotherm peaks with no shoulders, multiple peaks or discontinuous steps and those which are n^{th} order, of which, thermoset curing reactions are not as they are considered autocatalytic.[32] Calculations for the epoxy resin were not performed.

CONCLUSIONS

Materials selected for WFW applications must have desirable end-use properties as well as known in-process characteristics to define process control methods. For thermoset resins, both are dependent on environmental conditions, such as time and temperature, which affect the conversion or extent of cross-linking. Using the Kissinger, FWO and other methods, models of these relationships were utilized to estimate the kinetic parameters activation energy (E_a) and pre-exponential factor (A) to compare an epoxy, resole phenol, and cyanate ester resin system for WFW. Thermogravimetric data and the Borchardt and Daniels method did not provide expected values potentially due to the use of data from decomposition instead of curing reactions and unsuitability for thermoset/autocatalytic systems, respectively. Parameters calculated from exothermic peak data increased between the epoxy and resole phenol, with the cyanate ester having the highest. Values determined using the Kissinger and FWO methods were also in agreement within each resin, suggesting their applicability in future studies of similar systems.

REFERENCES

(1) *Articles – Fibear*. https://fibear.fi/articles/ (accessed 2025-05-07).

(2) Rinde, J. A.; Mones, E. T.; Newey, H. A. Filament Winding Epoxy Resins for Elevated Temperature Service.

(3) *A Guide to Controlling Filament Winding Parameters*. https://www.addcomposites.com/post/a-guide-to-controlling-filament-winding-parameters (accessed 2025-05-08).

(4) Strasser, C.; Moukhina, D. E.; Schmölzer, D. S. Kinetics Neo Software to Predict Curing Reactions.

(5) Puhurcuoğlu, N.; Arman, Y. Parameter Estimation of Epoxy Resin Cure Kinetics by Dynamics DSC Data. *Polym. Adv. Technol.* **2024**, *35* (7), e6498. https://doi.org/10.1002/pat.6498.

(6) Pace_Lexie_Polymer_Winter_2025 (LA-UR-25-22613).

(7) Larson, B. J.; Singh, M. Filament Winding: Efficient Material, Machinery & Process Decisions. YouTube, September 3, 2020.

(8) *O.O.A. Systems - ASC Process Systems*. http://www.aschome.com/index.php/en/ooa-ovens (accessed 2025-05-21).

(9) Composites, T. A. *Application of Out of Autoclave (OOA) Composite Prepregs*. AZoM. https://www.azom.com/article.aspx?ArticleID=7970 (accessed 2025-05-21).

(10) Fiber-Reinforced Polymer Composite Material Selection. NASA Lessons Learned. https://llis.nasa.gov/lesson/689 (accessed 2025-05-09).

(11) Ellis, B. *Chemistry and Technology of Epoxy Resins*; Springer, 2012.

(12) Sharma, D. A. *Understanding Epoxy Outgassing: Causes and Effects*. https://scivast.com/articles/understanding-epoxy-outgassing-causes-effects/ (accessed 2025-05-13).

(13) *Q & A: How to Properly Cure an Epoxy for the Aerospace Industry | MasterBond.com*. https://www.masterbond.com/q-and-a/how-properly-cure-epoxy-aerospace-industry (accessed 2025-05-21).

(14) Odian, G. G. *Principles of Polymerization*, Fourth edition.; Wiley: Hoboken, N.J, 2004. https://doi.org/10.1002/047147875X.

(15) Chow, S.; Steiner, P. R. Comparisons of the Cure of Phenol–Formaldehyde Novolac and Resol Systems by Differential Scanning Calorimetry. *J. Appl. Polym. Sci.* **1979**, *23* (7), 1973–1985. https://doi.org/10.1002/app.1979.070230708.

(16) Zhang, J.; Mei, G.; Xie, Z.; Zhao, S. Curing Mechanism of Phenolic Resin Binder for Oxide-Carbon Refractories. *ISIJ Int.* **2016**, *56* (1), 44–49. https://doi.org/10.2355/isijinternational.ISIJINT-2015-260.

(17) Gotro, J. *Beyond Epoxy: High Performance Thermosets Part Four – Cyanate Esters*. Polymer Innovation Blog. https://polymerinnovationblog.com/beyond-epoxy-high-performance-thermosets-part-four-cyanate-esters/ (accessed 2025-05-12).

(18) Klosterman, D. Preparation, Cure, and Characterization of Cyanate Ester-Epoxy Blends. In *SAMPE 2022*; NA SAMPE, 2022. https://doi.org/10.33599/nasampe/s.22.0797.

(19) Standard Test Method Fo Decomposition Kinetics by Thermogravimetry Using the Ozawa/Flynn/Wall Method.

(20) Standard Test Method for Thermal Stability of Chemicals by Differential Scanning Calorimetry. ASTM E537 – 24.

(21) Wang, X.-M.; Riedl, B.; Christiansen, A. W.; Geimer, R. L. Differential Scanning Calorimetry of the Effects of Temperature and Humidity on Phenol-Formaldehyde Resin Cure. *Polymer* **1994**, *35* (26), 5685–5692. https://doi.org/10.1016/S0032-3861(05)80042-4.

(22) Interpreting Unexpected Events and Transitions in DSC Results. TA Instruments. TA039.

(23) Hong, S.; Yeh, C. Catalytic Effects of Copper Oxides on the Curing and Degradation Reactions of Cyanate Ester Resin. *J. Appl. Polym. Sci.* **2007**, *104* (1), 442–448. https://doi.org/10.1002/app.25547.

(24) Wang, Y.; Hong, Y.; Hong, J. Cure Kinetics of a Flexible Aromatic Dicyanate with Schiff Base Structure. *J. Appl. Polym. Sci.* **1995**, *58* (9), 1585–1592. https://doi.org/10.1002/app.1995.070580922.

(25) Gómez, C. M.; Recalde, I. B.; Mondragon, I. Kinetic Parameters of a Cyanate Ester Resin Catalyzed with Different Proportions of Nonylphenol and Cobalt Acetylacetonate Catalyst. *Eur. Polym. J.* **2005**, *41* (11), 2734–2741. https://doi.org/10.1016/j.eurpolymj.2005.05.005.

(26) Szeluga, U.; Moryc, P. Curing of Dicyanate Ester/Epoxy Copolymers Modified with Polysiloxane and Butadiene-Acrylonitrile Rubbers. *J. Therm. Anal. Calorim.* **2012**, *109* (1), 73–80. https://doi.org/10.1007/s10973-011-1717-0.

(27) Gotro, J. *Practical Tips for Curing Thermosets Part Two: Impact of Cure Temperature on the Glass Transition Temperature*. Polymer Innovation Blog. https://polymerinnovationblog.com/practical-tips-curing-thermosets-part-two-impact-cure-temperature-final-tg/ (accessed 2025-05-12).

(28) Standard Test Method for Determination of Kinetic Parameters and Reaction Order for Thermally Unstable Materials by Differential Scanning Calorimetry Using the Kissinger and Farjas Methods. ASTM E2890 – 21.

(29) Zhou, D.; Du, S.; Yu, L.; Liu, Z. Nonisothermal Curing of a Solid Resole Phenolic Resin. *J. Appl. Polym. Sci.* **2011**, *121* (4), 1938–1945. https://doi.org/10.1002/app.33775.

(30) Standard Test Method for Kinetic Parameters for Thermally Unstable Materials Using Differential Scanning Calorimetry and the Flynn/Wall/Ozawa Method. ASTM E1641 – 23.

(31) Myers, G. E.; Christiansen, A. W.; Geimer, R. L.; Follensbee, R. A.; Koutsky, J. A. Phenol–Formaldehyde Resin Curing and Bonding in Steam-injection Pressing. I. Resin Synthesis, Characterization, and Cure Behavior. *J. Appl. Polym. Sci.* **1991**, *43* (2), 237–250. https://doi.org/10.1002/app.1991.070430203.

(32) Standard Test Method for Estimating Kinetic Parameters by Differential Scanning Calorimeter Using the Borchardt and Daniels Method. ASTM E2041 – 23.